

Atomic surface structure of the phosphorous-terminated InP(001) grown by MOVPE

P. Vogt*

Institut für Festkörperphysik, Technische Universität Berlin, Hardenbergstrasse 36, D-10623 Berlin, Germany

Th. Hannappel and S. Visbeck

Hahn-Meitner Institut, Glienicker Strasse 100, D-14109 Berlin, Germany

K. Knorr

Institut für Festkörperphysik, Technische Universität Berlin, Hardenbergstrasse 36, D-10623 Berlin, Germany

and Hahn-Meitner Institut, Glienicker Strasse 100, D-14109 Berlin, Germany

N. Esser and W. Richter

Institut für Festkörperphysik, Technische Universität Berlin, Hardenbergstrasse 36, D-10623 Berlin, Germany

(Received 20 May 1999)

Scanning tunneling microscopy (STM) was used to investigate the microscopic structure of the phosphorous (P)-rich so-called (2×1) reconstruction of InP(001). The samples were homoepitaxially grown in a commercial metal-organic vapor phase epitaxy reactor and then transferred under ultra high vacuum (UHV) conditions into a separate UHV-chamber equipped with low-energy electron diffraction (LEED) and scanning tunneling microscopy (STM). After transfer LEED patterns show a $(2 \times 1)/(2 \times 2)$ periodicity with streaks in the $[\bar{1}10]$ direction. STM images display rows in the $[110]$ direction formed by randomly distributed $(2 \times 2)/c(2 \times 2)/c(4 \times 2)$ -like local structures plus many defects. This disorder effect explains the (2×1) -like LEED pattern. The structure of the rows is interpreted in terms of P dimers directed along the $[110]$ direction which are adsorbed on a complete P layer underneath. Prolonged annealing at 350°C causes successive desorption of single P dimers as monitored by STM. The LEED pattern remains essentially unaffected and STM images with atomic resolution reveal zig-zag chains in the $[110]$ direction separated by twice the lattice constant. Two adjacent rows can be in or out of phase thus resulting in either $p(2 \times 2)$ or $c(4 \times 2)$ reconstructions. The structure of the rows can be explained in terms of buckled P dimers oriented along the $[\bar{1}10]$ direction on a complete In layer. [S0163-1829(99)51532-4]

The atomic structure of the InP(001) surfaces is poorly understood in comparison to the GaAs(001) surfaces which have been intensively studied during the last decade. As a result, GaAs(001) surface structures have often been regarded as the model surfaces explaining the structural aspects for other III-V compound (001) surfaces as well. Accordingly, indium (In)-rich (4×1) , (4×2) , and $c(8 \times 2)$ reconstructions have been assumed to be formed on InP(001) surfaces prepared by ion sputtering and annealing.¹⁻³ More recently, however, we demonstrated that the most In-rich stable InP surface is a (2×4) reconstruction terminated by In-P mixed dimers,⁴ a structure not observed on GaAs(001). Subsequently, this In-rich (2×4) surface reconstruction has been investigated, especially in terms of atomic surface structure.^{5,6} Other P-rich surface reconstructions, however, require a variation of surface stoichiometry.

In fact, under molecular-beam epitaxy (MBE) as well as under chemical-beam epitaxy (CBE) conditions P-rich (2×1) , (2×2) and In-rich (2×4) patterns have been observed *in situ* by reflection high-energy electron diffraction (RHEED).^{7,8} More recently a weak $c(4 \times 4)$ reconstruction prepared by MBE (Ref. 9) as well as by metal-organic vapor phase epitaxy (MOVPE) (Ref. 10) was reported. In this study we investigate the P-rich surfaces of InP(001).

The problem for surface analysis arises because of the incompatibility between the growth environment (especially

in the case of MOVPE) and the UHV conditions required for surface analysis. One way to overcome this incompatibility is to passivate the MOVPE grown InP samples by a thick amorphous P/As double-cap after growth which protects the surface during transport and which can be easily removed in UHV by thermal desorption at a temperature of approximately 400°C .¹¹ However, only the (2×4) reconstruction on InP(001) has been achieved in this way, indicating that the decapping temperature is too high to obtain the P-rich $c(4 \times 4)$, (2×1) , and (2×2) reconstructions. Alternatively, MOVPE grown samples can be directly analyzed if transfer from the growth reactor to an analysis chamber under UHV conditions is possible. In this case no further treatment of the surface is necessary, and hence many different reconstructions, both P-rich and In-rich, may be investigated.

The samples studied here were grown in a commercial AIX 200 MOVPE system with tertiarybutylphosphine (TBP), trimethylindium (TMIn), and diethylzinc (DEZn) as precursors. The Zn-doped ($p = 5 \times 10^{17} \text{ cm}^{-3}$) InP buffer layer was grown on Zn-doped ($p = 2 \times 10^{18} \text{ cm}^{-3}$) epitaxially grown InP(001) substrate held at 600°C , with a growth rate of $1.8 \mu\text{m/h}$. During cooling of the sample the TBP flow was switched off at a temperature of 350°C . Transfer of the P-rich InP surfaces was obtained in an apparatus custom-designed to produce UHV from MOVPE conditions in less than 20 s enabling the transfer in a mobile UHV vessel (5

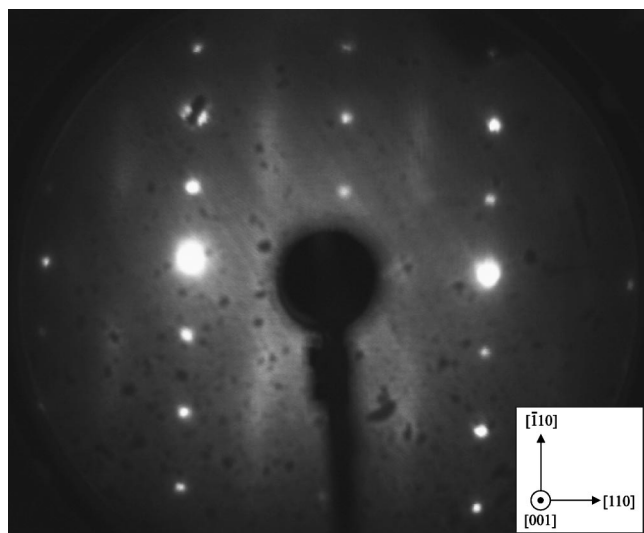


FIG. 1. $(2\times 1)/(2\times 2)$ -LEED pattern observed after transfer of the InP(001) sample. The $(2\times)$ periodicity lies along the $[\bar{1}10]$ direction, the $(\times 2)$ along the $[110]$ direction. The streaks extend along the $[110]$ direction. The pattern is obtained at an electron energy of 30 eV at room temperature.

$\times 10^{-10}$ mbar).¹² Thereafter the mobile vessel was connected to an UHV surface analysis chamber equipped with LEED and STM. The samples were transferred at a pressure below 5×10^{-8} mbar and the transfer took approximately 5 min. All measurements were performed at a base pressure of approximately 2×10^{-10} mbar. Auger electron spectroscopy (AES) data, recorded after transfer, reveal no detectable oxygen or carbon contamination.¹² LEED patterns were recorded using a four-grid reverse view LEED optics equipped with a digital video camera. Here we note that the $(n\times m)$ LEED notations for the patterns given later correspond to an n -fold symmetry along the $[\bar{1}10]$ and an m -fold symmetry along the $[110]$ direction. The STM images were taken in constant current mode. The bias values refer to the sample voltage with respect to the STM tip. During the experiments the temperature of the samples was measured with a well calibrated thermocouple in contact with the sample holder.

Immediately after transfer a $(2\times 1)/(2\times 2)$ LEED pattern was observed (Fig. 1). The (2×1) spots appear intense and are accompanied by $(n\times 2)$ streaks along the $[\bar{1}10]$ direction. After LEED measurements for approximately 20 min the streaks became more diffuse and finally vanished completely, thus leading to a (2×1) -like pattern. This behavior already indicates that a (2×1) -like pattern refers to a non-ideally ordered surface.

Figure 2 shows a large-scale STM image (500×480 Å²) of the sample after transfer. The image is taken at a sample bias of -5.2 V, and thus only filled surface states contribute. The surface appears atomically flat over the scanning range of the STM. Rowlike structures with additional corrugation along the rows appear in the $[110]$ direction. The single rows show many breaks and defects (dark areas) and are separated by 5 or 10 Å corresponding to one or two surface lattice constants in the $[\bar{1}10]$ direction, respectively. In Fig. 3 a high resolution STM image (60×60 Å²) is shown. The corrugation of the rows is clearly

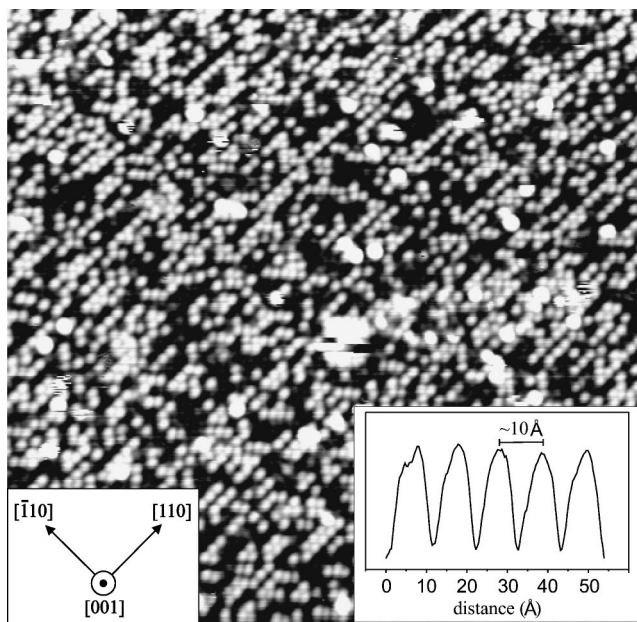


FIG. 2. Filled state STM image obtained after transfer of the InP(001) sample. The scan area is 500×480 Å, sample bias -5.2 V. The bright rows extending along the $[\bar{1}10]$ direction are separated by 5 Å and 10 Å corresponding to one and two lattice constants. The inset shows a line scan along one of the rows in the $[110]$ direction.

resolved in the image. The rows consist of symmetric oval structures which are allocated in a strict twofold periodicity along the $[110]$ direction, i.e., always separated by 10 Å (see inset Fig. 2). This result points strongly to the fact that each protrusion should consist of two equivalent atoms, i.e.,

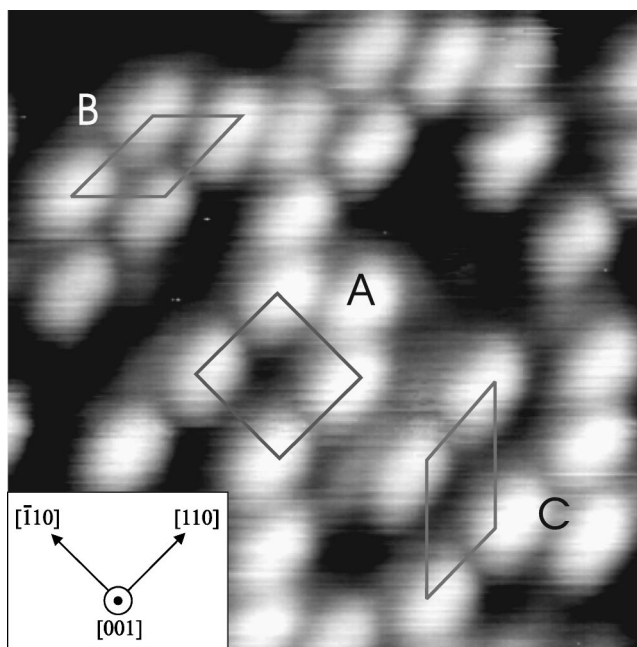


FIG. 3. High-resolution filled state STM image, scan area 60×60 Å, sample bias -5.5 V. Corrugation maxima in the bright rows are clearly resolved, separated by 10 Å, corresponding to the twofold lattice constant. As indicated, (2×2) (A), $c(2\times 2)$ (B), and $c(4\times 2)$ (C) regions exist on the InP(001) surface.

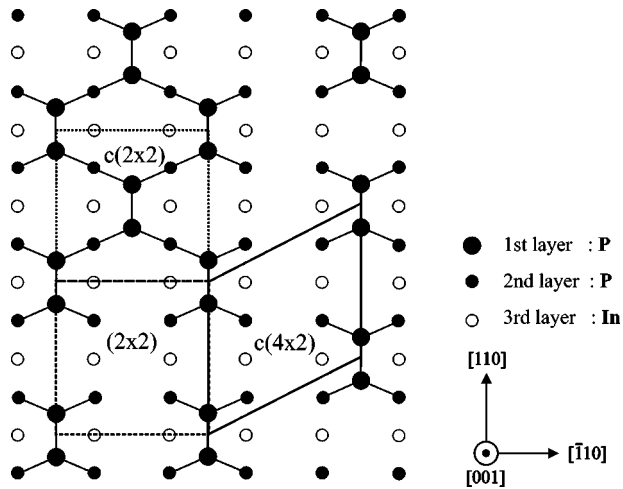


FIG. 4. Schematic model of the (2×2) , $c(2 \times 2)$, and $c(4 \times 2)$ arrangements on the InP(001) surface.

dimers. As clearly seen in Fig. 3 mainly three different local arrangements of the oval features, (2×2) (A), $c(2 \times 2)$ (B), and $c(4 \times 2)$ (C), can be found on the surface. These individual arrangements are more or less randomly distributed on the surface and do not form domains of a single prominent reconstruction. The coverage of the top layer is incomplete, or, in other words, the density of defects is very high, resulting in a poor long range ordering. It is also found that the defect density can differ dependent on the position on the surface as well as for different samples.

The STM results are in agreement with the LEED pattern since the latter corresponds to a superposition of a (2×2) , $c(2 \times 2)$, and $c(4 \times 2)$ periodicity. Growth conditions in agreement with photoemission data¹³ refer to P-rich surface conditions. Thus taking the STM results into account, the oval features in the high resolution STM image can be interpreted as P dimers which are oriented along the $[110]$ direction and hence bonded on top of another complete P layer (P dimers formed on an In layer would be oriented along the $[\bar{1}10]$ direction). This interpretation is also supported by annealing experiments which demonstrate that after desorbing the top layer another P-rich surface forms underneath (see below). In Fig. 4 a schematic model of the surface is shown presenting the three local structures found. All three structures in this model would not satisfy the electron-counting-rule which had to be applied for well ordered surfaces. For a (2×2) and a $c(4 \times 2)$ reconstruction there would be a lack of two electrons per unit cell whereas for a $c(2 \times 2)$ reconstruction the unit cell would contain an excess of two electrons. This may explain the occurrence of the three different local structures and the many defects rather than a well ordered reconstruction at the surface.

Prolonged annealing of the sample at 350°C leads to successive desorption of single P dimers as monitored by STM. At areas where the top P dimers are depleted, the evolution of another structure in the layer underneath can be seen. In Fig. 5 an STM image of the sample after annealing for approximately 3 h (350°C) is shown. The top P layer has completely vanished. The image reveals zig-zag chains along the $[110]$ direction separated by twice the surface lattice constant. The corrugation of the single chains also displays a

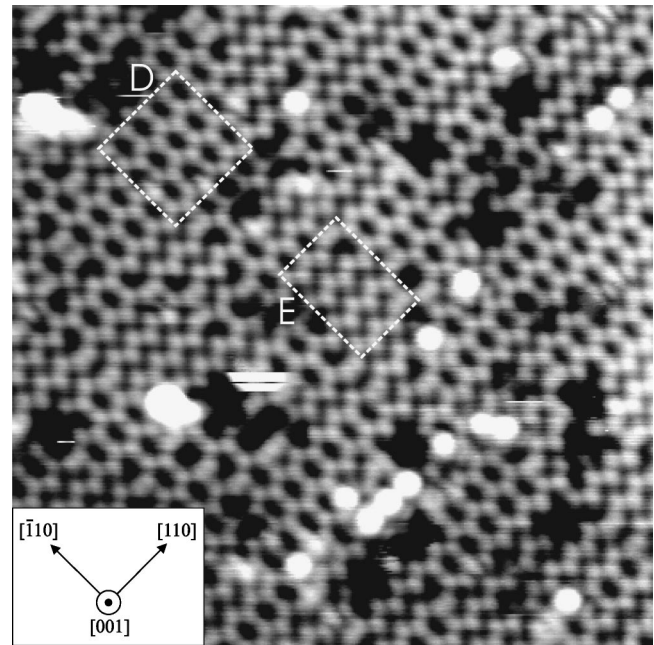


FIG. 5. High-resolution filled state STM image obtained after prolonged annealing of the InP(001) surface (scan area $200 \times 200 \text{ \AA}$, sample bias -5.2 V). The dashed areas show the $c(4 \times 2)$ (D) and $p(2 \times 2)$ (E) arrangements on the surface.

twofold symmetry in the $[\bar{1}10]$ direction. It can be clearly seen from the image that two adjacent rows can be in or out of phase resulting in $p(2 \times 2)$ (E) and $c(4 \times 2)$ (D) ('honeycomb') arrangements which through superposition explain the LEED pattern. It is also seen that there is no regular sequence of these arrangements, thus causing formation of streaks in the LEED pattern. The STM and LEED images resemble the ones obtained on Si(001) where buckled dimers are known to be formed.¹⁴ The structure of the rows can thus be inevitably explained by either asymmetric P-P or mixed In-P dimers. These results are in agreement with a recent report¹⁵ in which the same reconstruction for InP(001) was found. Observation of dimer-flipping conclusively rules out the In-P mixed dimer as an explanation for the structure. Hence we suggest an asymmetric P dimer model, which could refer either to buckled P dimers or an electronic inequivalence of the two P atoms. Within the model proposed by Li *et al.*¹⁵ one of the two P atoms of each dimer has a completely filled dangling bond. Thus in the filled state STM image only the P with the filled dangling bond is visible. Due to the formation of the dimers both of the atoms involved move slightly towards the center of the (1×1) unit mesh. For this reason distances between the atoms of two adjacent rows do not have a distance of a multiple integer of the lattice constant. This is also found in the STM image (Fig. 5).

Annealing to a higher temperature of 380°C leads already to the formation of the familiar In-rich (2×4) LEED pattern. This result explains why the preparation of a P-rich InP(001) reconstruction by thermal desorption of an As/P cap (400°C) is not possible. Further annealing to higher temperatures produces a degradation of the surface and accordingly the intensities of the (2×4) LEED spots decrease as the background signal increases. No other In-rich surface

reconstruction was observed by the annealing process. This is in agreement with our previous results on decapped InP(001) where the (2×4) is the most In-rich stable surface reconstruction.⁴

In conclusion, we have investigated MOVPE grown InP(001) surfaces by LEED and STM under UHV conditions. We were able to obtain atomically resolved STM images of the clean so called (2×1) reconstruction demonstrating that this surface is not a regular reconstructed structure but consists of coexisting (2×2) , $c(2 \times 2)$ and $c(4 \times 2)$ local structures. The single structures are explained in terms of differently arranged P dimers on top of a complete second P layer. The long-range order is strongly disrupted by missing dimers. Prolonged annealing at 350 °C leads to the desorption of the P dimers of the top layer and

the formation of a well ordered $p(2 \times 2)/c(4 \times 2)$ reconstruction in the P layer underneath. The zig-zag rows of which this reconstruction consists are explained in terms of asymmetric P-P dimers, consistent with Ref. 15. The temperature for the phase transition to the (2×4) reconstruction is found to be at approximately 380 °C. We have demonstrated that the UHV transport of MOVPE grown samples is possible and a suitable method to prepare clean, well defined III-V (001) surfaces.

We acknowledge the technical support of K. Lüdge and E. Eder during the STM experiments and valuable discussions with A.M. Frisch and M. Pristovsek. This work was financially supported by the DFG under Contract No. Es127/4-1.

*Author to whom correspondence should be addressed. FAX: ++49-30-314-21769. Electronic address: patrick@gift.physik.tu-berlin.de

¹C.R. Bayliss and D.L. Kirk, *J. Phys. D* **9**, 233 (1976).

²W. Weiss, R. Hornstein, D. Schmeisser, and W. Göpel, *J. Vac. Sci. Technol. B* **8**, 715 (1990).

³S. Riese, E. Milas, and H. Merz, *Surf. Sci.* **269/270**, 833 (1992).

⁴W.G. Schmidt, F. Bechstedt, N. Esser, M. Pristovsek, Ch. Schultz, and W. Richter, *Phys. Rev. B* **57**, 14 596 (1998).

⁵N. Esser, U. Resch-Esser, M. Pristovsek, and W. Richter, *Phys. Rev. B* **53**, R13 257 (1996).

⁶C.D. MacPherson, R.A. Wolkow, C.E.J. Mitchell, and A.B. McLean, *Phys. Rev. Lett.* **77**, 691 (1996).

⁷B.X. Yang and H. Hasegawa, *Jpn. J. Appl. Phys.* **33**, 742 (1994).

⁸B. Junno, S. Jeppesen, M.S. Miller, and L. Samuelson, *J. Cryst. Growth* **164**, 66 (1996).

⁹K.B. Ozanyan, P.J. Parbrook, M. Hopkins, C.R. Whitehouse, Z. Sobiesierski, and D.I. Westwood, *J. Appl. Phys.* **82**, 474 (1997).

¹⁰M. Zorn, T. Trepk, J.-T. Zettler, B. Junno, C. Meyne, K. Knorr, T. Wethkamp, M. Klein, M. Miller, W. Richter, and L. Samuelson, *Appl. Phys. A: Mater. Sci. Process.* **65**, 333 (1997).

¹¹K. Knorr, M. Pristovsek, U. Resch-Esser, N. Esser, M. Zorn, and W. Richter, *J. Cryst. Growth* **170**, 230 (1997).

¹²Th. Hannappel, S. Visbeck, K. Knorr, J. Mahrt, M. Zorn and F. Willig, *Appl. Phys A* (to be published).

¹³P. Vogt, A.M. Frisch, Th. Hannappel, S. Visbeck, F. Willig, Ch. Jung, N. Esser, W. Braun, and W. Richter, *Phys. Status Solidi B* (to be published).

¹⁴R.A. Wolkow, *Phys. Rev. Lett.* **68**, 2636 (1992).

¹⁵L. Li, B.-K. Han, Q. Fu, and R.F. Hicks, *Phys. Rev. Lett.* **82**, 1879 (1999).